IEEE Access
Multidisciplinary : Rapid Review : Open Access Journal

Received December 23, 2019, accepted January 21, 2020, date of publication February 3, 2020, date of current version February 12, 2020.

Digital Object Identifier 10.1109/ACCESS.2020.2971177

A Novel ACFM Probe With Flexible Sensor Array for Pipe Cracks Inspection

JIANMING ZHAO, WEI LI, (Member, IEEE), JIANCHAO ZHAO, XIN'AN YUAN, YUKAI ZHU, AND ZHENXIANG WANG

Center for Offshore Engineering and Safety Technology, China University of Petroleum (East China), Qingdao 266580, China

Corresponding author: Wei Li (ronald8044@163.com)

This work was supported in part by the National Key Research and Development Program of China under Grant 2017YFC0804503, in part by the National Natural Science Foundation of China under Grant 51574276 and Grant 51675536, in part by the National Postdoctoral Program for Innovative Talents under Grant BX20190386, in part by the China Postdoctoral Science Foundation funded project under Grant 2019M662461, in part by the Major National Science and Technology Program under Grant 2016ZX05028-001-05, in part by the Fundamental Research Funds for the Central Universities under Grant 18CX05017A, and in part by the Post-Graduate Innovation Project of China University of Petroleum under Grant YCX2019063.

ABSTRACT Pipes are important components for well drilling, production, and transportation in petroleum industry. However, due to factors such as vibration, corrosion, fatigue damage, etc., pipes are prone to cracks. This paper presents a novel ACFM probe with flexible sensor array for the inspection of inner and outer cracks in pipes with different diameters. The simulation model of the ACFM probe with flexible sensor array is established by the finite element method. The influences of the crack length and the lift-off on the distance between the Bz peaks and troughs are analyzed respectively. The relationship between the offset distance of the crack from the pickup coil center and the detection sensitivity is studied. The probe made by flexible PCB and the testing system are developed. The experiments are carried out. The results of experiments and simulations show that the probe with flexible sensor array can detect inner and outer surface cracks for pipes with different diameters, and both circumferential and axial cracks can be identified. The distance between the Bz peaks and troughs can measure the crack length. When the crack is offset from the center of the pickup coil, the adjacent pickup coil can compensate for the detection sensitivity.

INDEX TERMS ACFM, flexible sensor array, pipe cracks inspection.

I. INTRODUCTION

Pipes such as drill pipes, risers, and pipelines et al. are important components for well drilling, production, and transportation in petroleum industry [1], [2]. However, due to the harsh service environment, it is prone to surface cracks on the inner and outer walls of the pipes [3]. What's more, cracks continue to expand in the presence of stress and corrosion, which will cause structural failure [4]. Therefore, regular inspection and evaluation of pipe cracks are necessary.

There are many detection methods for pipe cracks. Magnetic particle testing (MT) technology and penetrant flaw testing (PT) technology are the most commonly used non-destructive testing techniques, but they both need to remove the coatings and attachments on the pipe, which is time-consuming and costly. Magnetic flux leakage (MFL) detection technology can only detect ferromagnetic pipes [5], [6]. Ultrasonic testing (UT) technology requires coupling mediums and it is not sensitive to surface cracks [7]. Eddy current (EC) detection technology is a conventional electromagnetic non-destructive testing technology. It uses a higher excitation frequency to induce a circular non-uniform current field on the surface of the specimen, which results in its signal being sensitive to lift-off [8].

Alternating current field measurement (ACFM) is an electromagnetic non-destructive testing technology, which has been widely recognized and accepted as one of the most reliable methods to detect surface-breaking cracks in metallic components [9]–[11]. ACFM induces a unidirectional current of uniform strength on the surface of the workpiece, which is different from the principle of EC [12], [13]. It has the advantages of insensitivity to lift-off and no need to remove structural surface coatings, which has been widely used in crack detection of rails, welds and underwater structures [14]–[16]. As a key part of the detection system, a series of researches have been carried out on the form of ACFM probes.

The associate editor coordinating the review of this manuscript and approving it for publication was Kai Li.

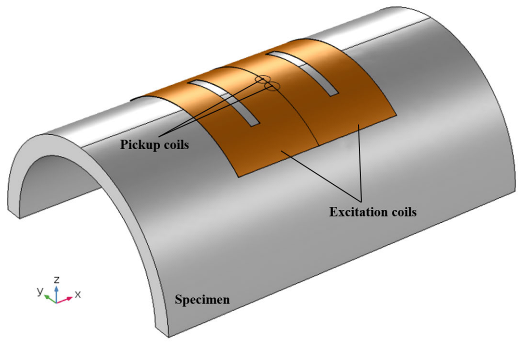

FIGURE 1. Simulation model.

The traditional ACFM probe uses a U-shaped magnetic core, so it is only suitable for the detection of flat metal structures [17]–[19]. When the workpiece being inspected is a pipe, it is difficult for the probe to induce a uniform current of stable intensity on the surface of the pipe. The commercial ACFM micropencil probe that is manufactured by TSC is used to size the subsurface section of multiple cracks and determine the propagation angle for non-vertical surface-breaking cracks in rail and wheels [10], [20]–[23]. However, the detection range of the micropencil probe is relatively small and the efficiency is relatively low. Li *et al.* proposed a feed-through ACFM probe with sensors array for pipe string cracks inspection [24]–[26]. Feng *et al.* presented an alternating current field measurement probe for pipeline inner inspection [27]. Ye *et al.* proposed a novel rotating current probe with GMR array sensors for steam generate tube inspection [28], [29]. But the above-mentioned pipe detection probes are only applicable to pipes of one diameter. For pipes of different diameters, the probe needs to be remade and it results in higher detection costs.

In this paper, a novel ACFM probe with flexible sensor array is presented for the detection of inner and outer cracks in pipes with different diameters. This paper is organized in the following way. In Section 2, the simulation model of the flexible probe is built by the finite element method. The influences of the crack length, the lift-off and the offset distance of the crack from the pickup coil center on characteristic signal are analyzed respectively. In Section 3, the probe and the testing system are built. And pipe specimens are tested. Conclusion and future work are outlined in Section 4.

II. FINITE ELEMENT METHOD MODEL

A. SIMULATION MODEL

The 3D FEM model of pipe cracks inspection is established by COMSOL Multiphysics and frequency domain magnetic response is chosen under the AC/DC module. The FEM model is shown in Fig. 1, which includes a specimen, excitation coils, and pickup coils. The excitation coils are composed of two symmetrical rectangular coils. The rectangular coil has 50 turns and the lift-off is 0.4 mm. Sinusoidal signals whose frequency is 1000 Hz and current is 0.3A are loaded on the two rectangular coils respectively. The pickup coils turn is 9. The center distance between two pickup coils is 7.15 mm and its lift-off is 0.2 mm. The detailed parameters of the model are shown in Table. 1.

TABLE 1. Parameters of the model.

Name	Value
Specimen	Aluminum, Outer diameter= 130 mm, Inside diameter= 110 mm
Excitation coils	Copper, Length = 90 mm, width = 90 mm, height = 0.2 mm
Pickup coils	Copper, Outer diameter= 7 mm, Inside diameter= 0.6 mm, height = 0.2 mm

The surface current density of the specimen is extracted as shown in Fig. 2. It can be seen from the figure that the excitation coil induces two symmetrical eddy current fields on the surface of the specimen, and the uniform electric field is generated in the middle of the two eddy current fields.

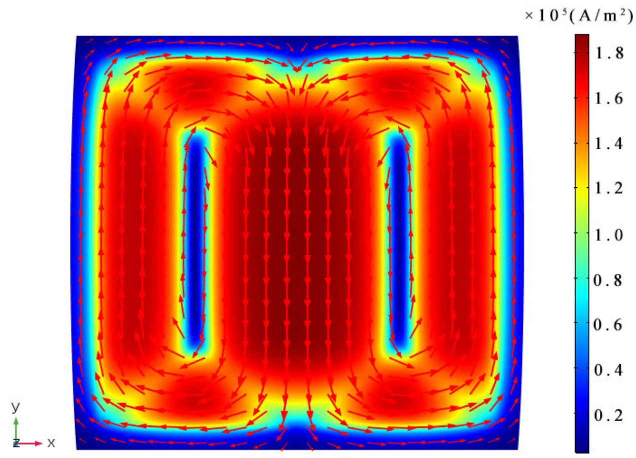

FIGURE 2. Surface current density.

B. ANALYSIS OF DISTORTED CURRENT

In order to explore the disturbance principle of the cracks on the uniform electromagnetic field, the electric field distribution of the crack on the surface of the specimen is simulated. The crack (length = 10mm, width = 0.2mm, depth = 2mm) is in the outer wall of the pipe, which is located in the middle of the excitation coils and perpendicular to the direction of the induced current.

The current distribution is extracted is shown in Fig. 3. It can be seen from Fig. 3a that when a crack exists, the surface current will bypass from both ends of the crack, one end is clockwise and the other end is counterclockwise. The current in the profile will bypass the bottom of the crack from Fig. 3b. The phenomena are consistent with the ACFM theory.

C. ANALYSIS OF CHARACTERISTIC SIGNALS

In order to obtain the relationship between the component of the magnetic field in the Z direction (Bz) and cracks of

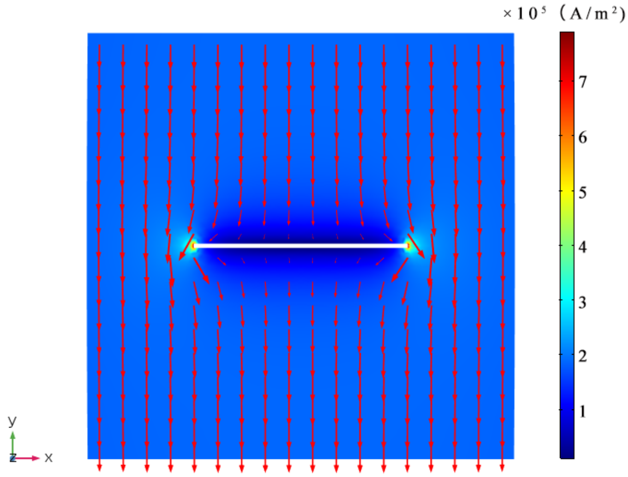

(a) surface current lines

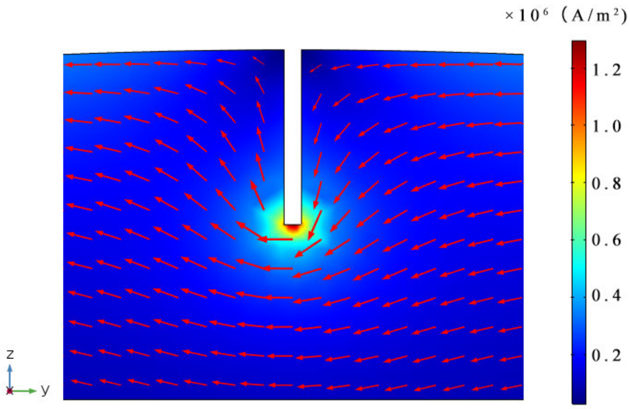

(b) profile current lines

FIGURE 3. **Current disturbance.**

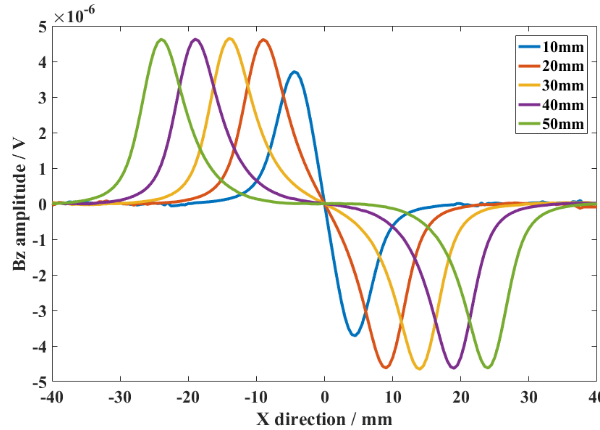

(a) *Bz* with different length cracks

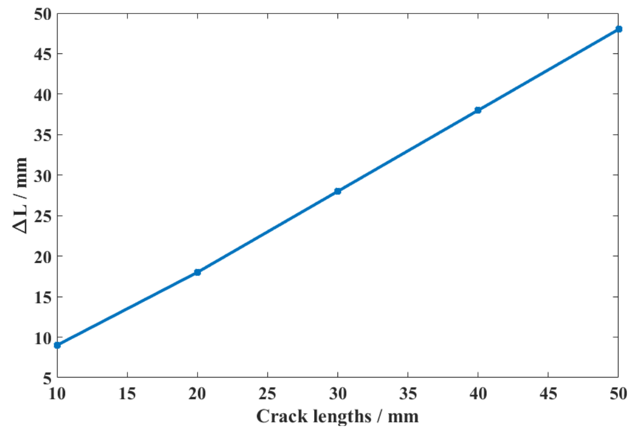

(b) *ΔL* with different length cracks

FIGURE 4. **Characteristic signal with different length cracks.**

different lengths, the cracks(depth 2 mm, width 0.2 mm) of different lengths (10 mm, 20 mm, 30 mm, 40 mm, 50 mm) is simulated by parameterized scanning. The Bz signals with cracks of different lengths are shown in Fig. 4a. If the crack length is relatively short, the crack length has an effect on the distance (ΔL) between the Bz peaks and troughs and distortion of it. When the crack length is relatively long, it only affects the ΔL. The relationship between the crack length and the ΔL is shown in Fig 4b. The length information is reflected by the ΔL. Due to the smaller lift-off of the sensor, the ΔL can more accurately reflect the crack length compared to the traditional U-shaped probe.

In order to investigate the effects of lift-off on ΔL, the probe at different lift-off are simulated, and the results are shown in Fig. 5. It shows that the ΔL becomes decreases as the lift-off increases. However, when the lift-off is increased by 3.8 mm, ΔL only changed by 0.6 mm. Lift-off has little effect on the ΔL.

Because the width of the crack is much smaller than the diameter of the pickup coil, the detection sensitivity is affected by the offset distance of the crack from the pickup coil center. Simulation analysis of cracks with different offset distances are shown in Fig. 6.

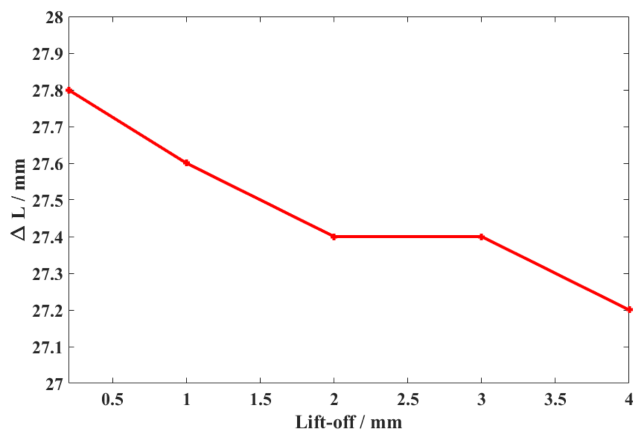

FIGURE 5. **ΔL with different lift-off.**

The farther the offset distance of the crack, the smaller the Bz distortion of the pickup coil A is shown in Fig. 7a, and the larger the Bz distortion of the pickup coil B is shown in Fig. 7b. The peak values of the two pickup coils (A and B) for the different offset distances are shown in Fig. 7c. It can be seen from the figure that the average value of the two pickup signal peaks remains almost unchanged for the different crack offset distances. It indicated

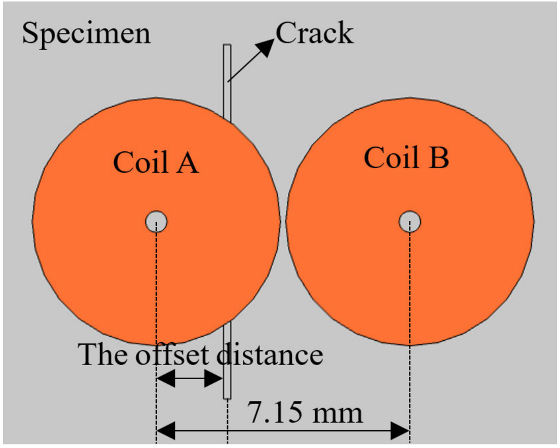

FIGURE 6. Simulation with the different offset distances.

that the adjacent pickup coil can compensate for the detection sensitivity when the crack is offset from the center of the pickup coil.

III. EXPERIMENTS

A. PROBE AND TESTING SYSTEM

The ACFM probe made by flexible PCB and the testing system are established, as shown in Fig. 8. The probe (length = 80 mm, width = 83mm) consists of excitation coils and pickup coils is shown in Fig. 8a. The excitation coils are composed of two symmetrically rectangular coils with 53 turns wire whose width is 0.2 mm. The spacing between wires is 0.15 mm. The probe has 7 pickup coils with the same wire width and distance as the excitation coils. Each pickup coils has 9 turns wires. The outer diameter of the pickup coil is 7 mm. The distance between each two adjacent excitation coils is 7.15 mm.

The testing system consists of a probe, an instrument, a computer and specimens is shown in Fig. 8b and Fig. 8c. The signal generator generates a sinusoidal signal, whose frequency is 1 KHz. The sinusoidal signal whose amplitude is 0.3 A is loaded on the excitation coils after power amplification. The pickup coils convert the changing magnetic field signal into a voltage signal. The voltage signal is filtered and amplified, then the output signal is converted into a DC signal by phase-locked amplification. The DC signal is digitized by a NI 6361 Capture card. Sample rate is 0.1 MS/s and sampling number is 1000. Digital signals are transmitted to a computer for processing.

B. EXPERIMENT ON CRACK INSIDE PIPE

The specimen is a ferromagnetic pipe (outer diameter = 130 mm, inside diameter = 110 mm) with an inner-wall circumferential crack (length = 30 mm, depth = 1.2 mm, width = 0.2 mm), as shown in Fig. 9a. The probe sweeps through the pipe, and the experimental results are shown in Fig. 9b. It can be seen from the figure that the probe with flexible sensor array can detect cracks inside the pipe. When cracks are present, the *Bz* signal shows a peak

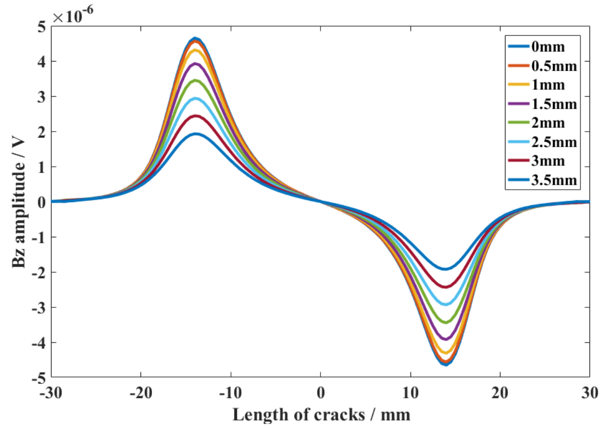

(a) *Bz* of pickup coil A with the different offset distances

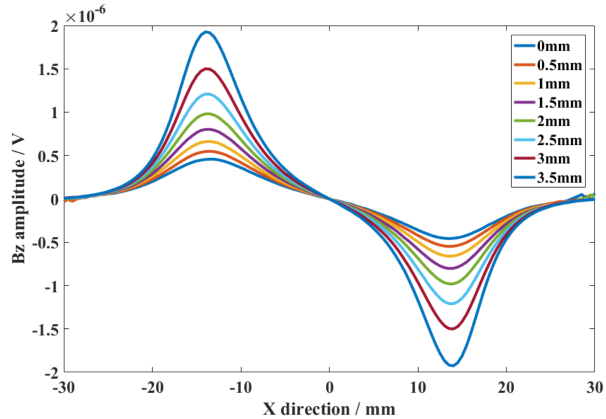

(b) *Bz* of pickup coil B with the different offset distances

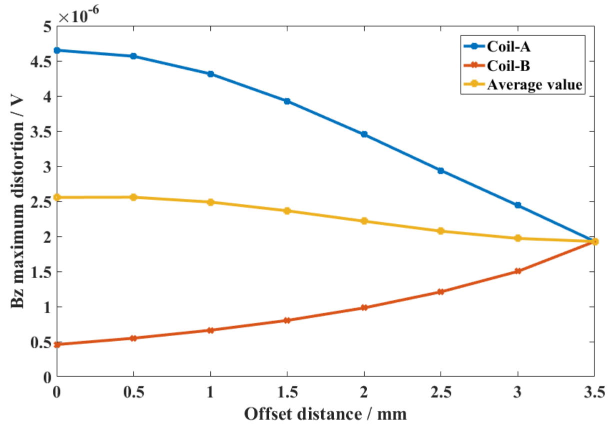

(c) Peak values of the two pickup coils (A and B) for the different offset distances

FIGURE 7. Characteristic signal with the different offset distances.

and a trough. The crack appears at a position below the channel 5.

C. EXPERIMENT ON CRACKS OUTSIDE PIPE

There are three axial cracks (depth = 4 mm, width = 0.5 mm) with different lengths (30 mm, 35 mm, 40 mm) outside the aluminum alloy pipe (outer diameter = 65 mm, inside diameter = 55 mm), as shown in Fig. 10a. The pipe is driven by the scanner (Fig. 8c) to pass through the probe

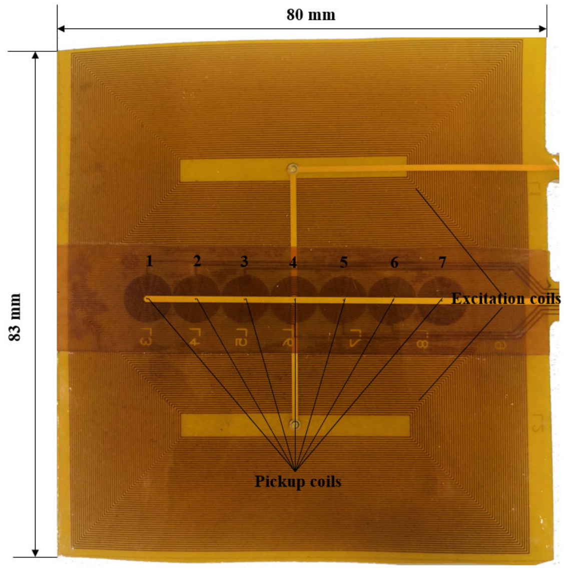

(a) Probe with flexible sensor array

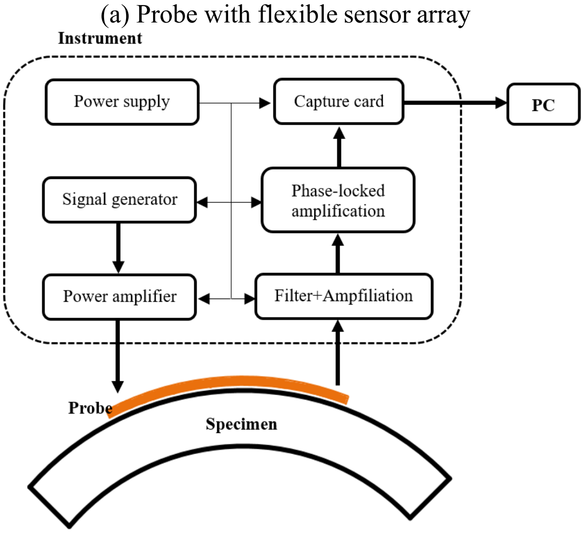

(b) Schematic diagram of the testing system

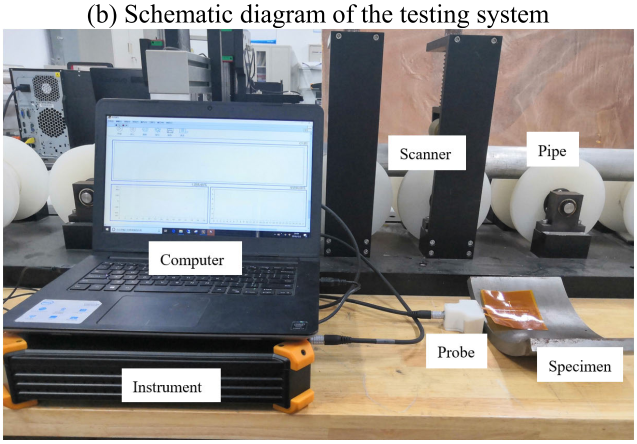

(c) Photo of the testing system

FIGURE 8. Probe and testing system.

at the speed of 5 mm/s. As shown in Fig. 10b, the space magnetic field around the cracks on the pipe is plotted. There are three peaks and troughs under the channel 4.

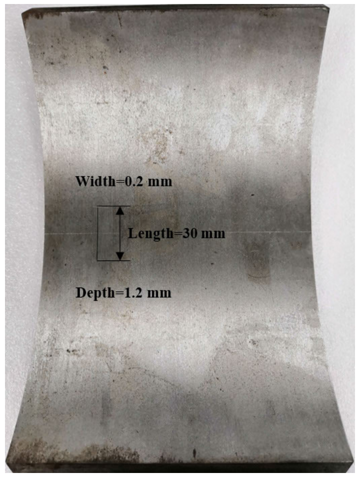

(a) Pipe with inner crack

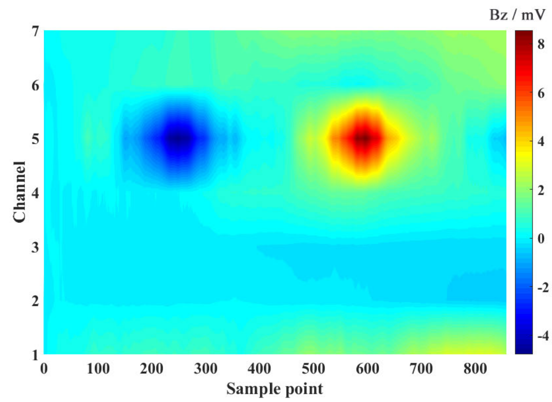

(b) Testing results

FIGURE 9. Test results with crack inside pipe.

TABLE 2. Results of different length cracks.

	No.1	No.2	NO.3
L/mm	40	35	30
ΔL	38.78	34.60	29.60
Error	3.05%	1.14%	1.33%

Therefore, theBz signal of channel 4 is independently plotted is shown in Fig. 10c. It shows that the longer the crack, the longer ΔL. The relationship between the crack length and ΔL is shown in Table. 2. The measuring error of the crack length is given in Eqs. (1).

$$Error = (L - \Delta L)/L \tag{1}$$

where L is the actual length of the crack, the ΔL is the distance between the Bz peaks and troughs and *Error* is the measuring error of the crack length.

It shows that ΔL is always shorter than the actual crack length, but the relative error is very small. The maximum error is only 3.05%. So ΔL can be used to measure the crack length, and the simulation results have been verified.

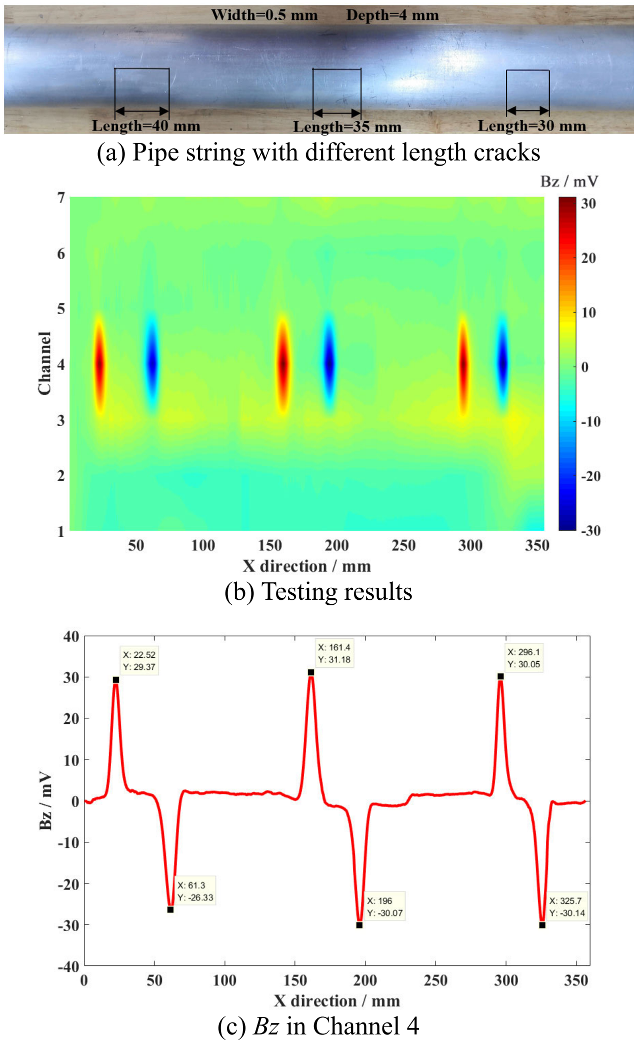

FIGURE 10. Test results with the pipe string.

IV. CONCLUSION AND FUTURE WORK

In this paper, we present a novel ACFM probe with flexible sensor array for the detection of inner and outer cracks in pipes with different diameters. The simulation model of the ACFM probe with flexible sensor array is established to study the disturbance principle of uniform electromagnetic field by finite element software COMSOL. The effects of crack length and the lift-off on ΔL are analyzed respectively. And the influences of the offset distance of the crack from the pickup coil center on detection sensitivity are explored. The flexible ACFM probe and the testing systems are established. The pipes with different diameters are detected. The results show the excitation coils can induce a uniform electromagnetic field on the surface of the test specimen. The further the crack is offset from the center of the pickup coil, the smaller the Bz distortion of the pickup coil. But when the crack is offset from the center of the detection coil, the adjacent pickup coil can compensate for the detection sensitivity. The flexible ACFM probe can detect both inner and outer surface cracks in pipes with different diameters, and both circumferential and axial cracks can be identified. The ΔL reflects the length information of the crack. Lift-off has little effect on the ΔL. Further work will focus on the detection and evaluation of other type defects.

ACKNOWLEDGMENT

The authors would like to thank the experimental equipment provided by the Center for Offshore Engineering and Safety Technology, China University of Petroleum (East China), located in Shandong province of China.

REFERENCES

[1] A. K. Das, "The present and the future of line pipe steels for petroleum industry," *Mater. Manuf. Process.*, vol. 25, nos. 1–3, pp. 14–19, Mar. 2010.
[2] N. Y. Ibragimov and E. N. Ibragimova, "Investigation of geometric parameters of cracks in silicate enamel coatings of steel pipes," *Chem. Petroleum Eng*, vol. 54, nos. 1–2, pp. 107–109, May 2018.
[3] S. Abedi, A. Abdolmaleki, and N. Adibi, "Failure analysis of SCC and SRB induced cracking of a transmission oil products pipeline," *Eng. Failure Anal.*, vol. 14, no. 1, pp. 250–261, Jan. 2007.
[4] S. Yu, P. Yuan, K. Deng, W. Liu, Y. Lin, and J. Zhuang, "Experimental and numerical study on the longitudinal-crack failure of double-shoulder tool joint," *Eng. Failure Anal.*, vol. 91, pp. 1–11, Sep. 2018.
[5] S. Kathirmani, A. Tangirala, S. Saha, and S. Mukhopadhyay, "Online data compression of MFL signals for pipeline inspection," *NDT & E Int.*, vol. 50, pp. 1–9, Sep. 2012.
[6] S. Liu, Y. Sun, L. He, X. Jiang, and Y. Kang, "Quantitative MFL characterization study in hard magnetic material surface topography measurement," *Measurement*, vol. 135, pp. 503–519, Mar. 2019.
[7] S. Zhang, C. Guo, L. Cheng, H. Wang, and R. Liao, "Testing method for composite insulators interface based on nonlinear ultrasonic," *IEEE Access*, vol. 7, pp. 83111–83119, 2019.
[8] Y. Du, S. Xie, X. Li, Z. Chen, T. Uchimoto, and T. Takagi, "A fast forward simulation scheme for eddy current testing of crack in a structure of carbon fiber reinforced polymer laminate," *IEEE Access*, vol. 7, pp. 152278–152288, 2019.
[9] B. Blakeley and M. Lugg, "ACFM: Application of ACFM for inspection through metal coatings," *Insight-Non-Destructive Test. Condition Monit.*, vol. 52, no. 6, pp. 310–315, 2010.
[10] H. Rowshandel, M. Papaelias, C. Roberts, and C. Davis, "Development of autonomous ACFM rail inspection techniques," *Insight-Non-Destructive Test. Condition Monit.*, vol. 53, no. 2, pp. 85–89, 2011.
[11] X. Yuan, W. Li, G. Chen, X. Yin, W. Yang, and J. Ge, "Two-step interpolation algorithm for measurement of longitudinal cracks on pipe strings using circumferential current field testing system," *IEEE Trans. Ind. Informat.*, vol. 14, no. 2, pp. 394–402, Feb. 2018.
[12] A. Raine and M. Lugg, "A review of the alternating current field measurement inspection technique," *Sensor Rev.*, vol. 19, no. 3, pp. 207–213, Sep. 1999.
[13] M. Ravan, S. Sadeghi, and R. Moini, "Neural network approach for determination of fatigue crack depth profile in a metal, using alternating current field measurement data," *IET Sci., Meas. Technol.*, vol. 2, no. 1, pp. 32–38, Jan. 2008.
[14] M. C. Lugg, "The first 20 years of the AC field measurement technique," in *Proc. Abstr. 17th World Conf. Non-Destructive Test.*, 2008, pp. 2034–2041.
[15] D. Topp, "Recent developments and applications of the ACFM inspection method and ASCM stress measurement method," *Non Destructive Test. Aust.*, vol. 42, no. 5, p. 143, 2005.
[16] F. C. R. Marques, M. V. M. Martins, and D. A. Topp, "Experiences in the use of ACFM for Offshore platform Inspection in Brazil," *Insight-Non-Destructive Test. Condition Monitor.*, vol. 43, no. 6, pp. 394–398, 2001.
[17] W. Zheng, L. Zhang, Y. Su, and T. Fang, "Optimization design of alternating current field measurement inducer," *Int. J. Appl. Electrom*, vol. 49, no. 1, pp. 133–143, Sep. 2015.
[18] L. Wei, C. Guoming, Y. Xiaokang, Z. Chuanrong, and L. Tao, "Analysis of the lift-off effect of a U-shaped ACFM system," *NDT & E Int.*, vol. 53, pp. 31–35, Jan. 2013.
[19] J. Ge, W. Li, G. Chen, X. Yin, Y. Wu, J. Liu, and X. Yuan, "Analysis of signals for inclined crack detection through alternating current field measurement with a U-shaped probe," *Insight-Non-Destructive Test. Condition Monitor.*, vol. 59, no. 3, pp. 121–128, 2017.

[20] H. Rowshandel, G. Nicholson, J. Shen, and C. Davis, "Characterisation of clustered cracks using an ACFM sensor and application of an artificial neural network," *NDT & E Int.*, vol. 98, pp. 80–88, Sep. 2018.

[21] G. L. Nicholson, H. Rowshandel, X. J. Hao, and C. L. Davis, "Measurement and modelling of ACFM response to multiple RCF cracks in rail and wheels," *Ironmaking Steelmaking*, vol. 40, no. 2, pp. 87–91, Feb. 2013.

[22] J. L. Shen, L. Zhou, H. Rowshandel, G. L. Nicholson, and C. L. Davis, "Determining the propagation angle for non-vertical surface-breaking cracks and its effect on crack sizing using an ACFM sensor," *Meas. Sci. Technol.*, vol. 26, no. 11, Nov. 2015, Art. no. 115604.

[23] J. M. C. Muñoz, F. G. Márquez, and M. Papaelias, "Railroad inspection based on ACFM employing a non-uniform B-spline approach," *Mech. Syst. Signal Process.*, vol. 40, no. 2, pp. 605–617, Nov. 2013.

[24] W. Li, X. Yuan, G. Chen, X. Yin, and J. Ge, "A feed-through ACFM probe with sensor array for pipe string cracks inspection," *NDT & E Int.*, vol. 67, pp. 17–23, Oct. 2014.

[25] X. Yuan, W. Li, G. Chen, X. Yin, and J. Ge, "Circumferential current field testing system with TMR sensor array for non-contact detection and estimation of cracks on power plant piping," *Sens. Actuators A, Phys.*, vol. 263, pp. 542–553, Aug. 2017.

[26] W. Li, X. Yuan, G. Chen, X. Yin, and J. Ge, "Induced circumferential current for transverse crack detection on a pipe string," *Insight-Non-Destructive Test. Condition Monitor.*, vol. 57, no. 9, pp. 528–533, Sep. 2015.

[27] Y. Feng, L. Zhang, and W. Zheng, "Simulation analysis and experimental study of an alternating current field measurement probe for pipeline inner inspection," *NDT & E Int.*, vol. 98, pp. 123–129, Sep. 2018.

[28] C. Ye, Y. Huang, L. Udpa, and S. S. Udpa, "Novel rotating current probe with GMR array sensors for steam generate tube inspection," *IEEE Sensors J.*, vol. 16, no. 12, pp. 4995–5002, Jun. 2016.

[29] C. Ye, J. Xin, Z. Su, L. Udpa, and S. S. Udpa, "Novel transceiver rotating field nondestructive inspection probe," *IEEE Trans. Magn.*, vol. 51, no. 7, pp. 1–6, Jul. 2015.

JIANMING ZHAO received the B.E. degree in mechanical design manufacture and automation from the China University of Petroleum, in 2017, where he is currently pursuing the Ph.D. degree in mechanical engineering.

WEI LI (Member, IEEE) received the Ph.D. degree in mechanical and electronics engineering from the China University of Petroleum, China, in 2007. He joined the China University of Petroleum, where he is currently a Professor of mechanical and electronics engineering.

JIANCHAO ZHAO received the B.E. degree in mechanical design manufacture and automation from the China University of Petroleum, in 2019, where he is currently pursuing the M.E. degree in mechanical engineering.

XIN'AN YUAN received the B.E. and M.E. degrees in mechanical design manufacture and automation from the China University of Petroleum, in 2013 and 2016, respectively, where he is currently pursuing the Ph.D. degree in mechanical engineering.

YUKAI ZHU received the B.E. degree in mechanical design manufacture and automation from the China University of Petroleum in 2018, where he is currently pursuing the M.E. degree in mechanical engineering.

ZHENXIANG WANG received the B.E. degree in mechanical design manufacture and automation from the China University of Petroleum, in 2018, where he is currently pursuing the M.E. degree in mechanical engineering.